

Supplemental Information

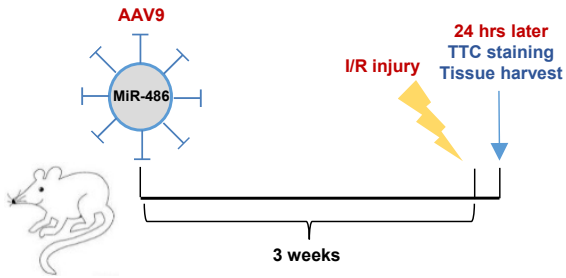
**miR-486 attenuates cardiac ischemia/reperfusion
injury and mediates the beneficial effect
of exercise for myocardial protection**

Yihua Bei, Dongchao Lu, Christian Bär, Shambhabi Chatterjee, Alessia Costa, Isabelle Riedel, Frank C. Mooren, Yujiao Zhu, Zhenzhen Huang, Meng Wei, Meiyu Hu, Sunyi Liu, Pujiao Yu, Kun Wang, Thomas Thum, and Junjie Xiao

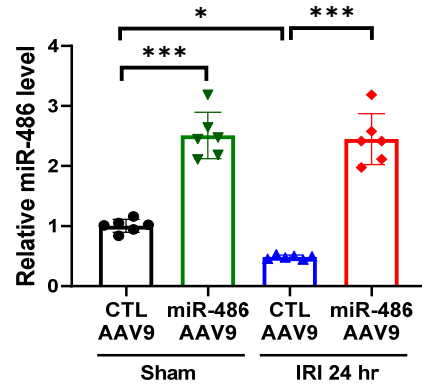
Supplemental Figures

Figure S1

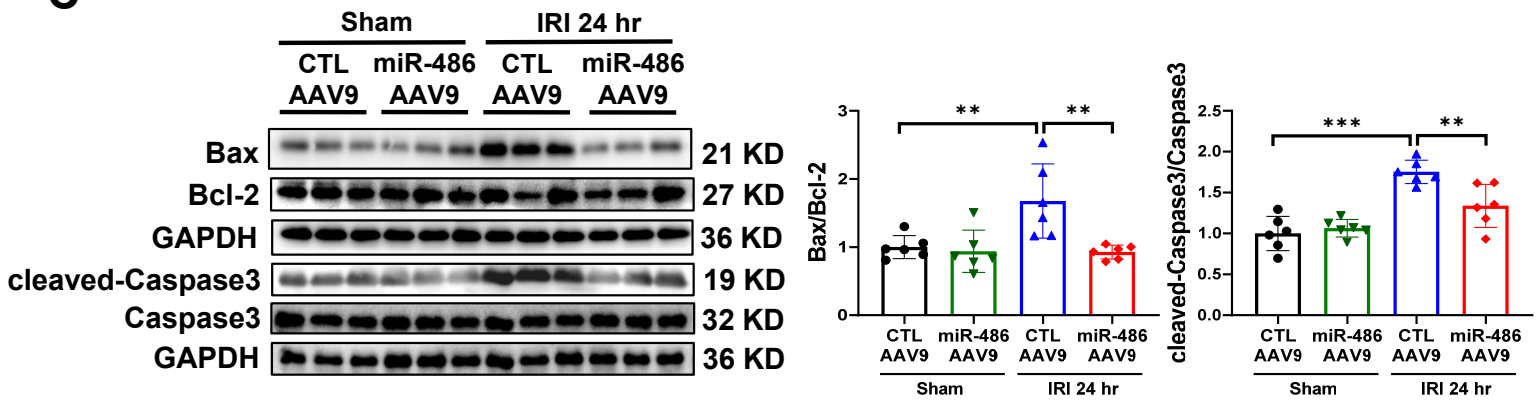
A



B



C



D

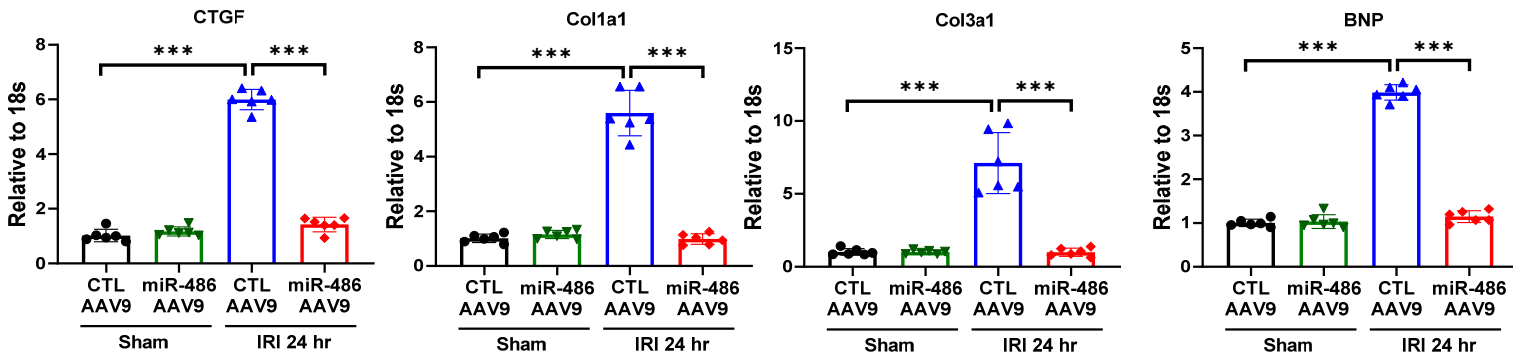
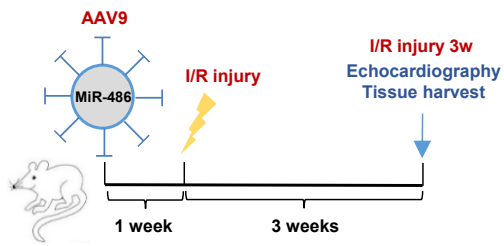
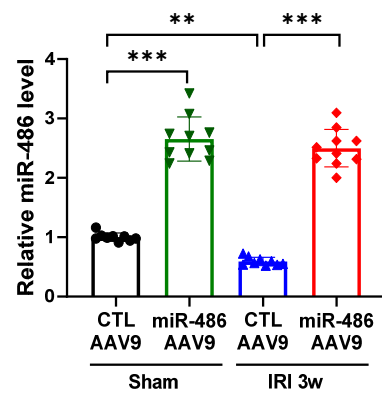


Figure S2

A



B



C

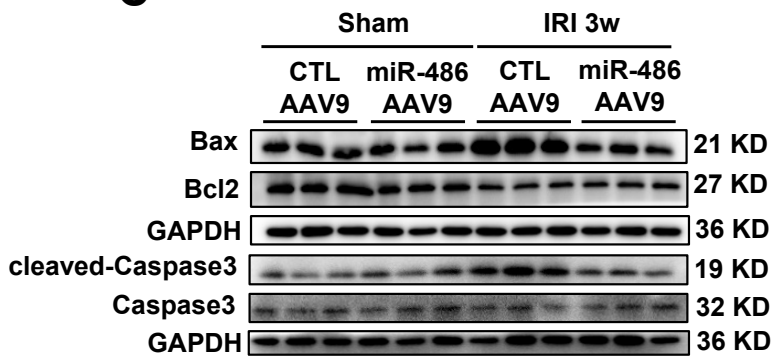
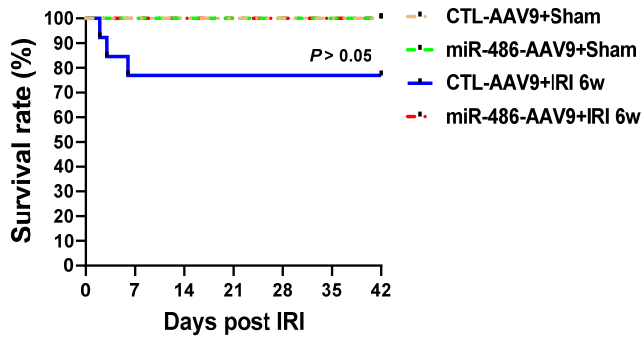
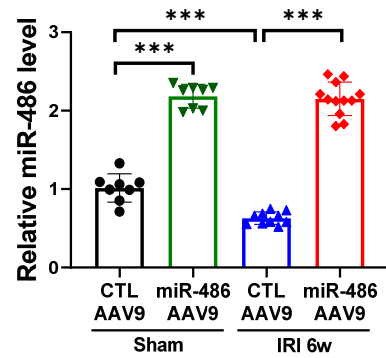


Figure S3

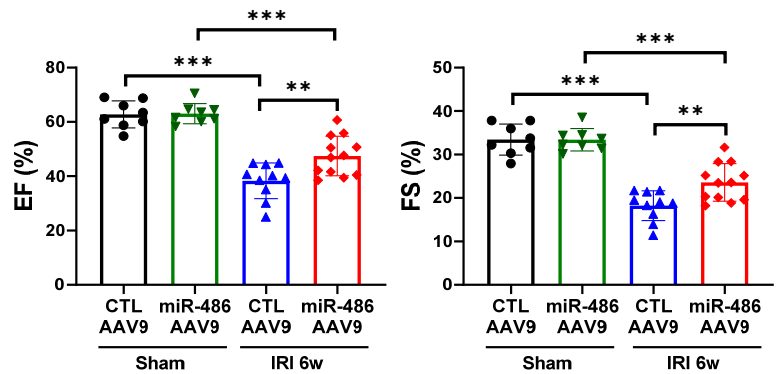
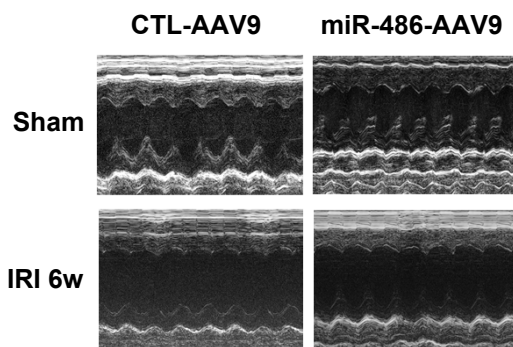
A



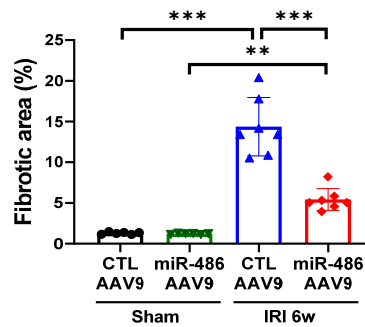
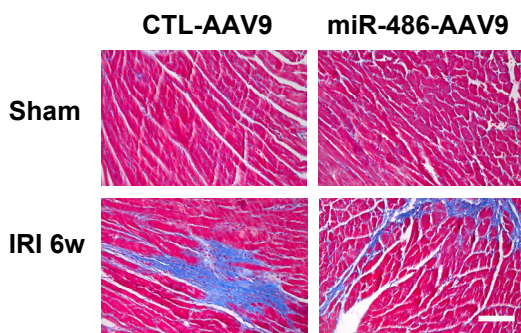
B



C



D



E

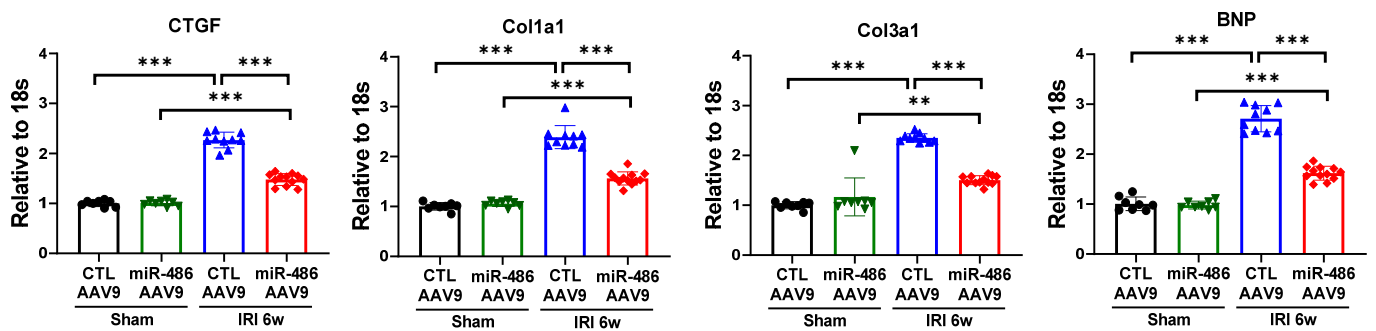
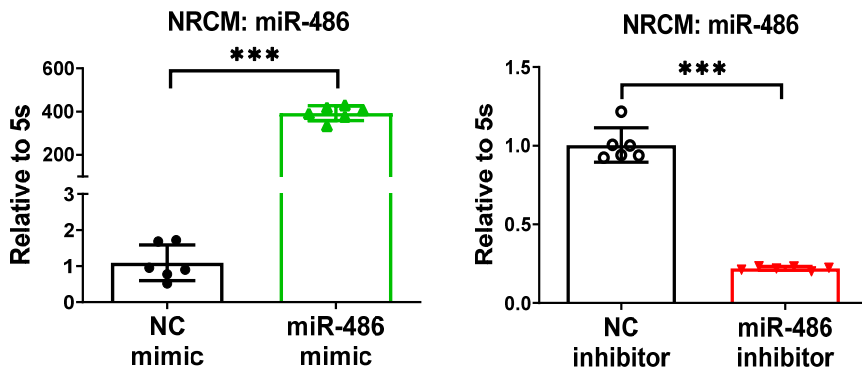


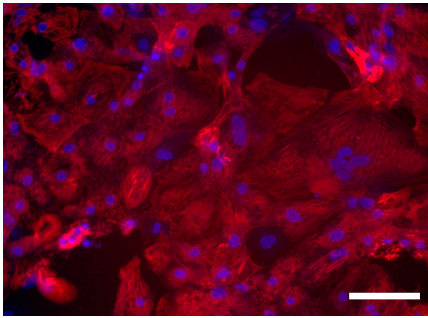
Figure S5

A



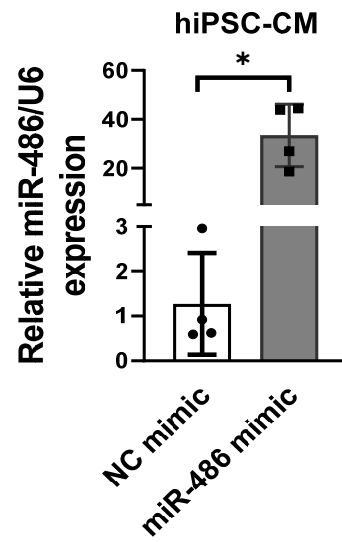
B

hiPSC-CM



cTNT+DAPI

C



D

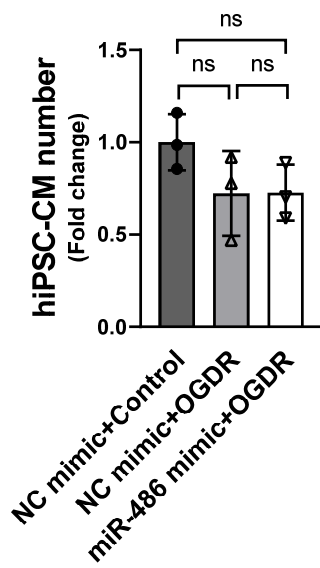


Figure S6

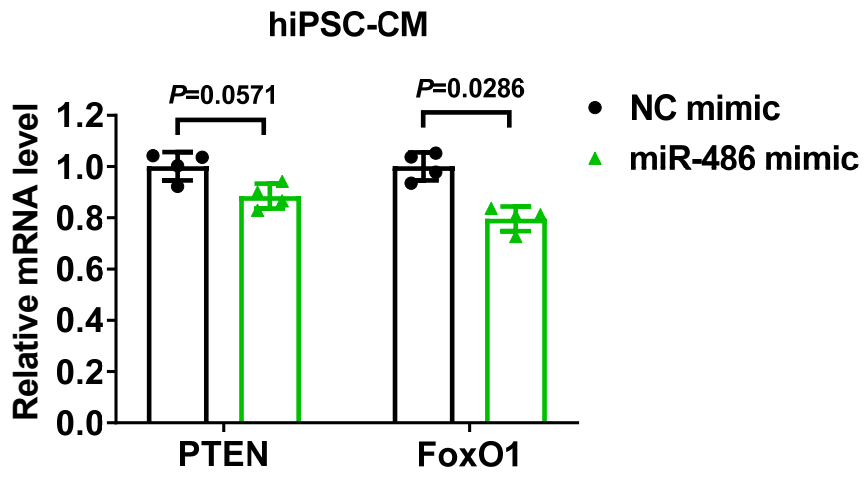
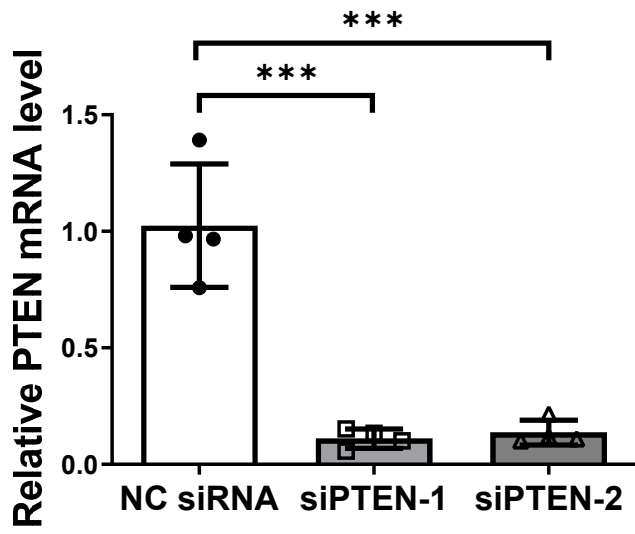


Figure S7

A



B

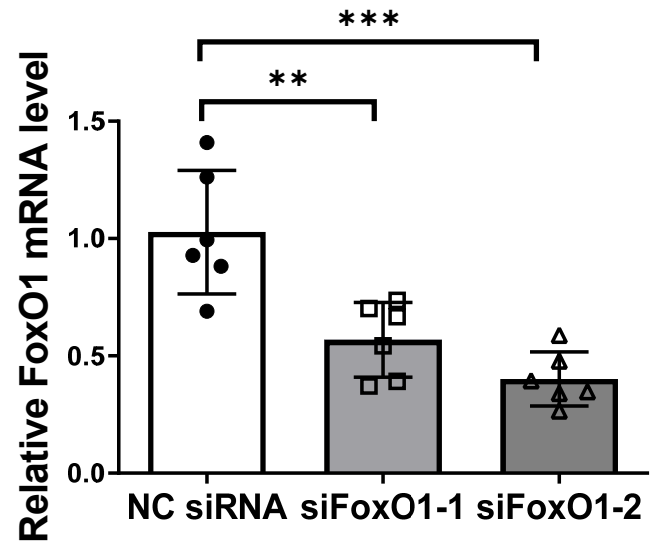


Figure S8

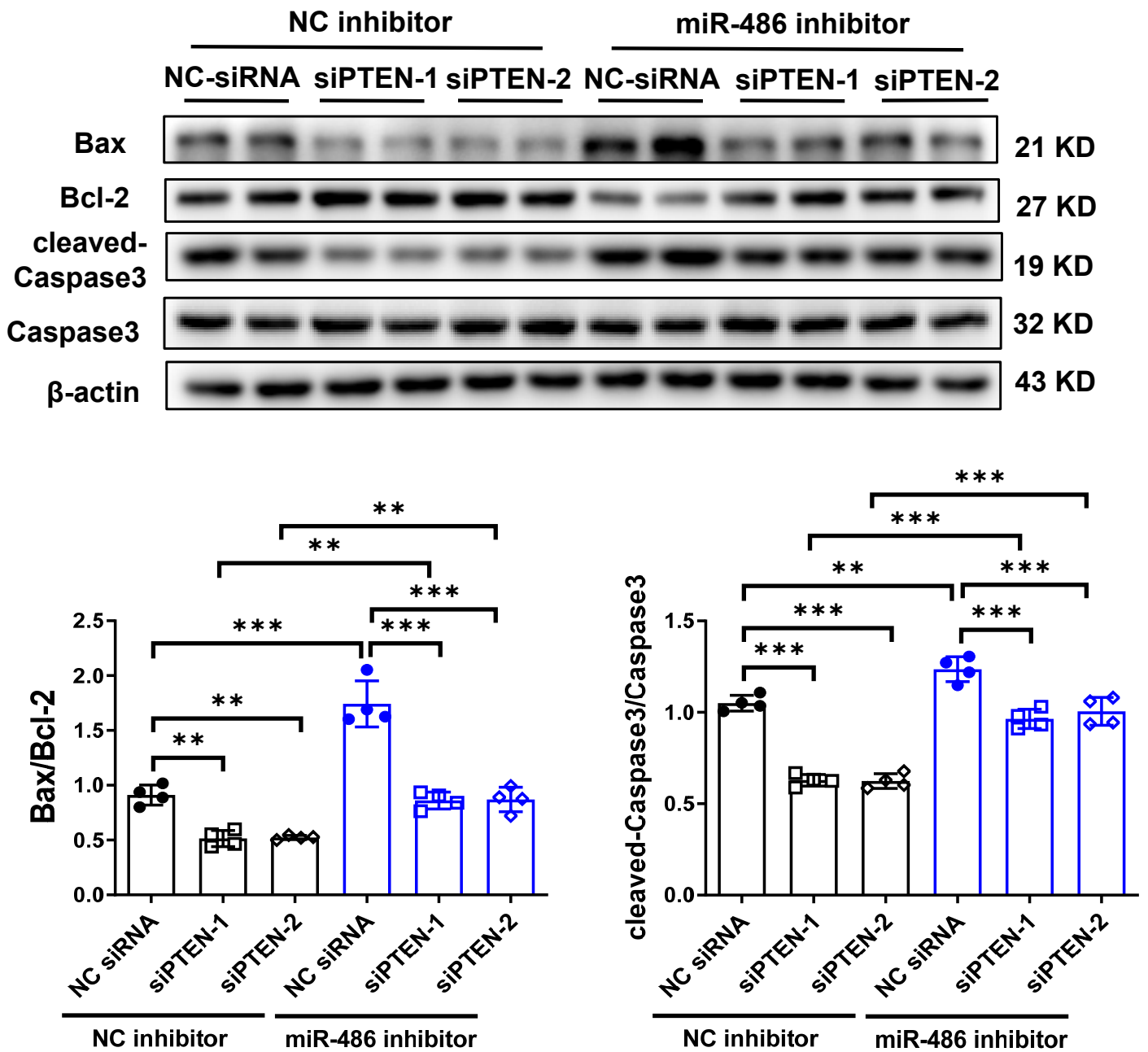


Figure S9

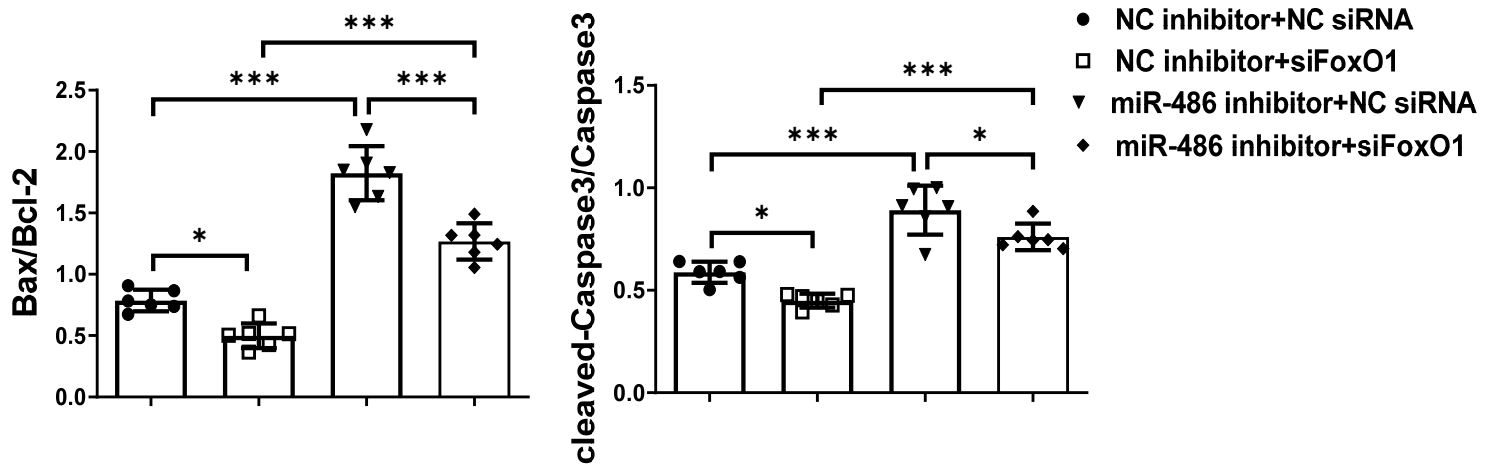
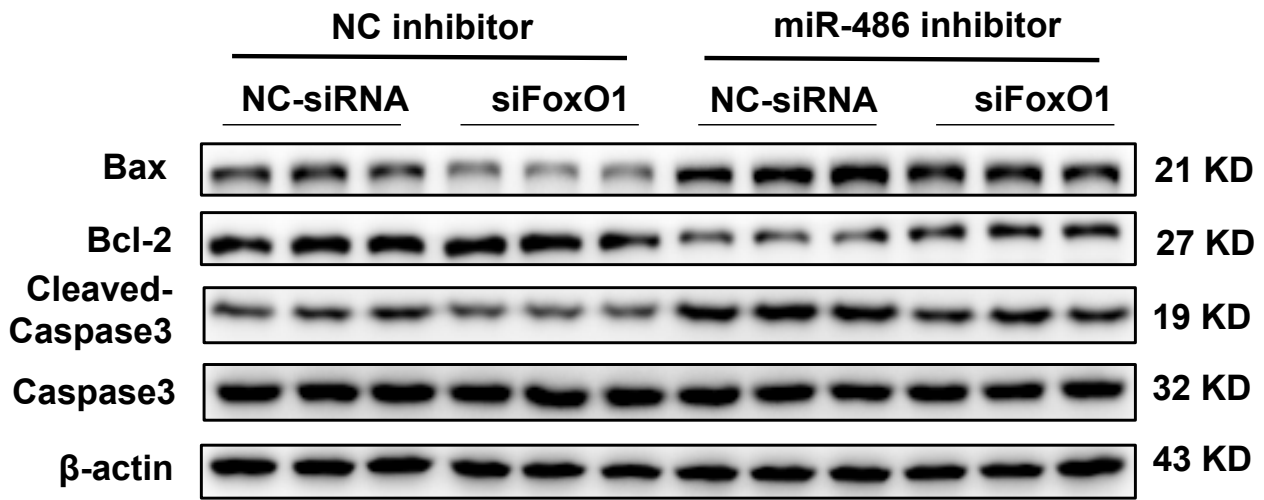
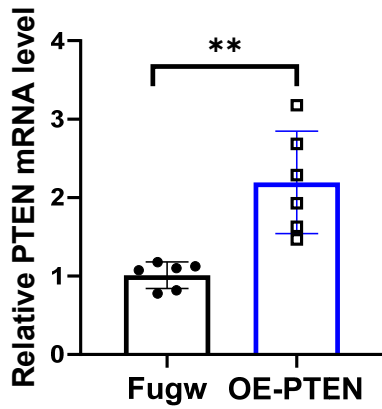
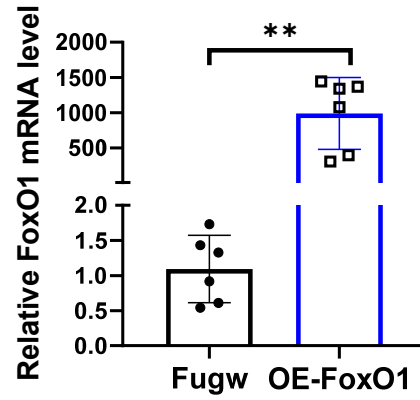


Figure S10

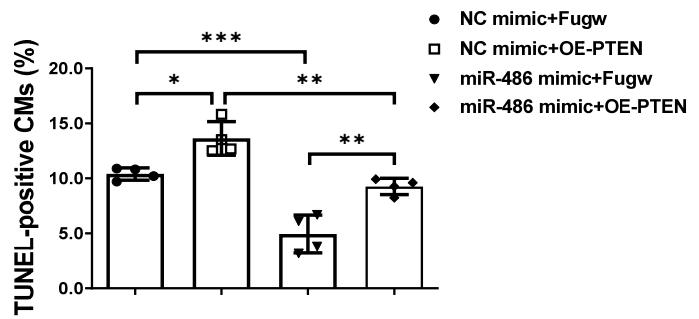
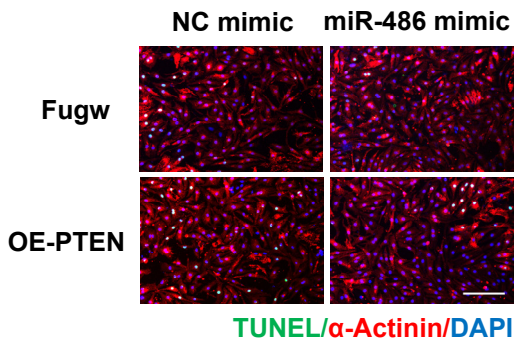
A



B



C



D

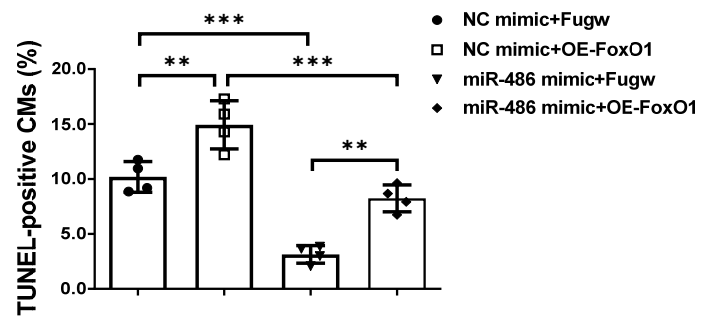
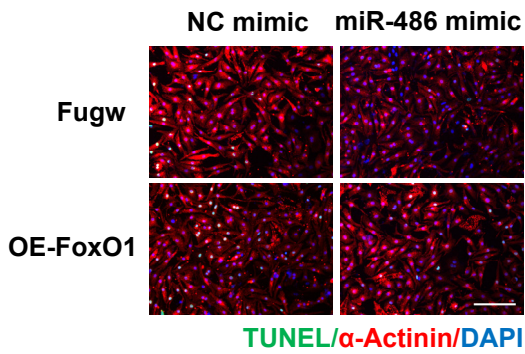
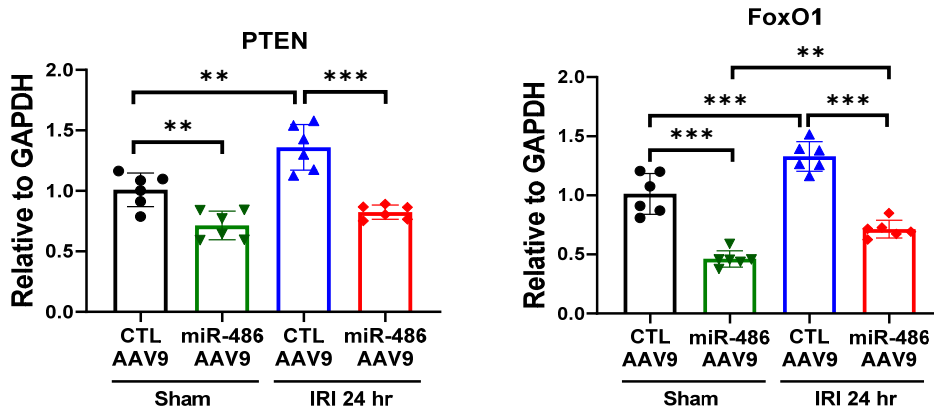
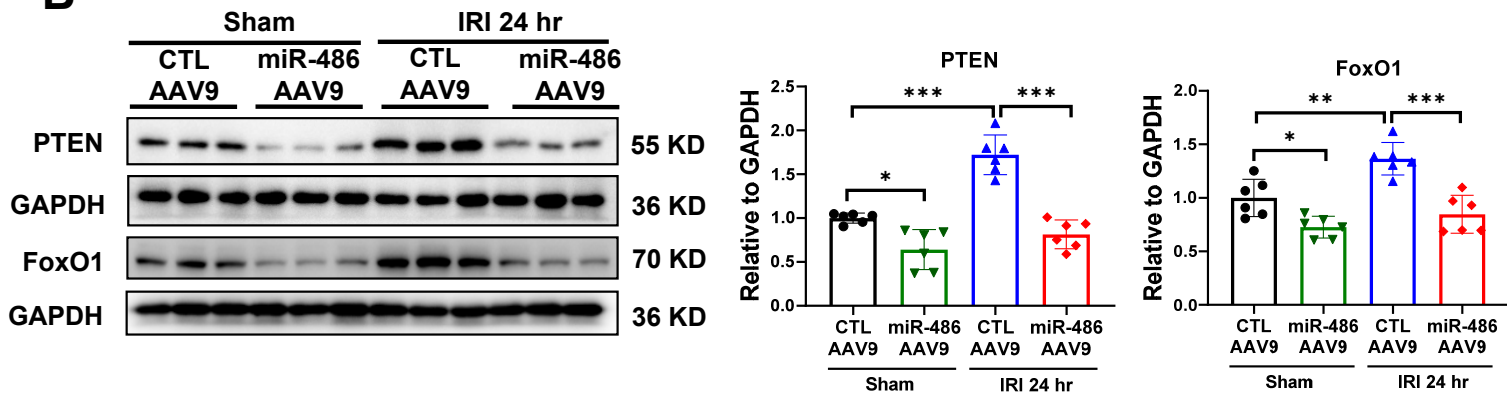


Figure S11

A



B



C

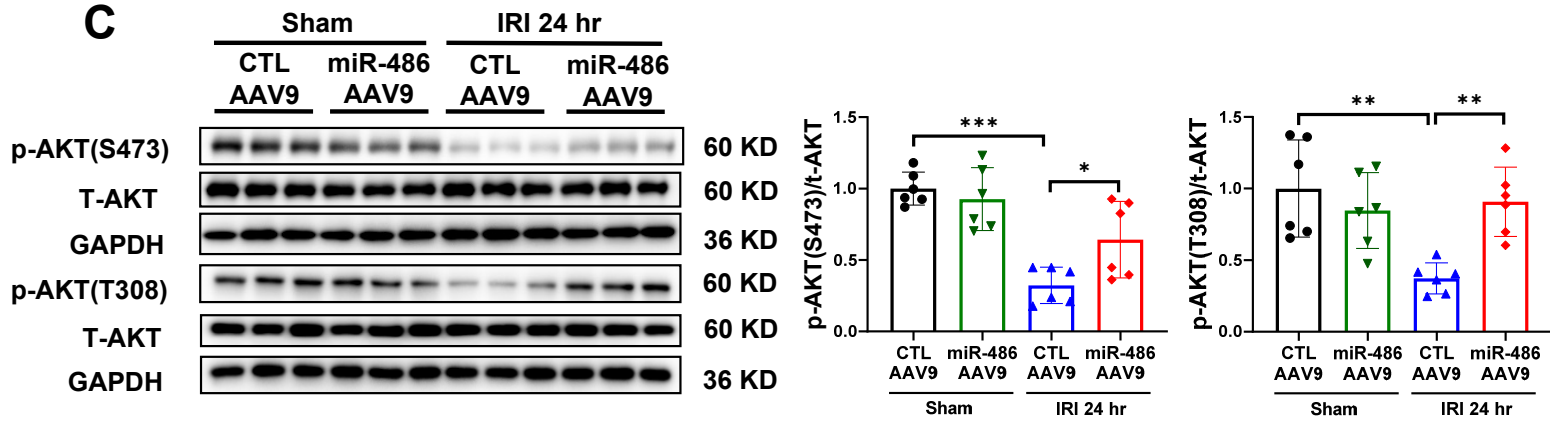
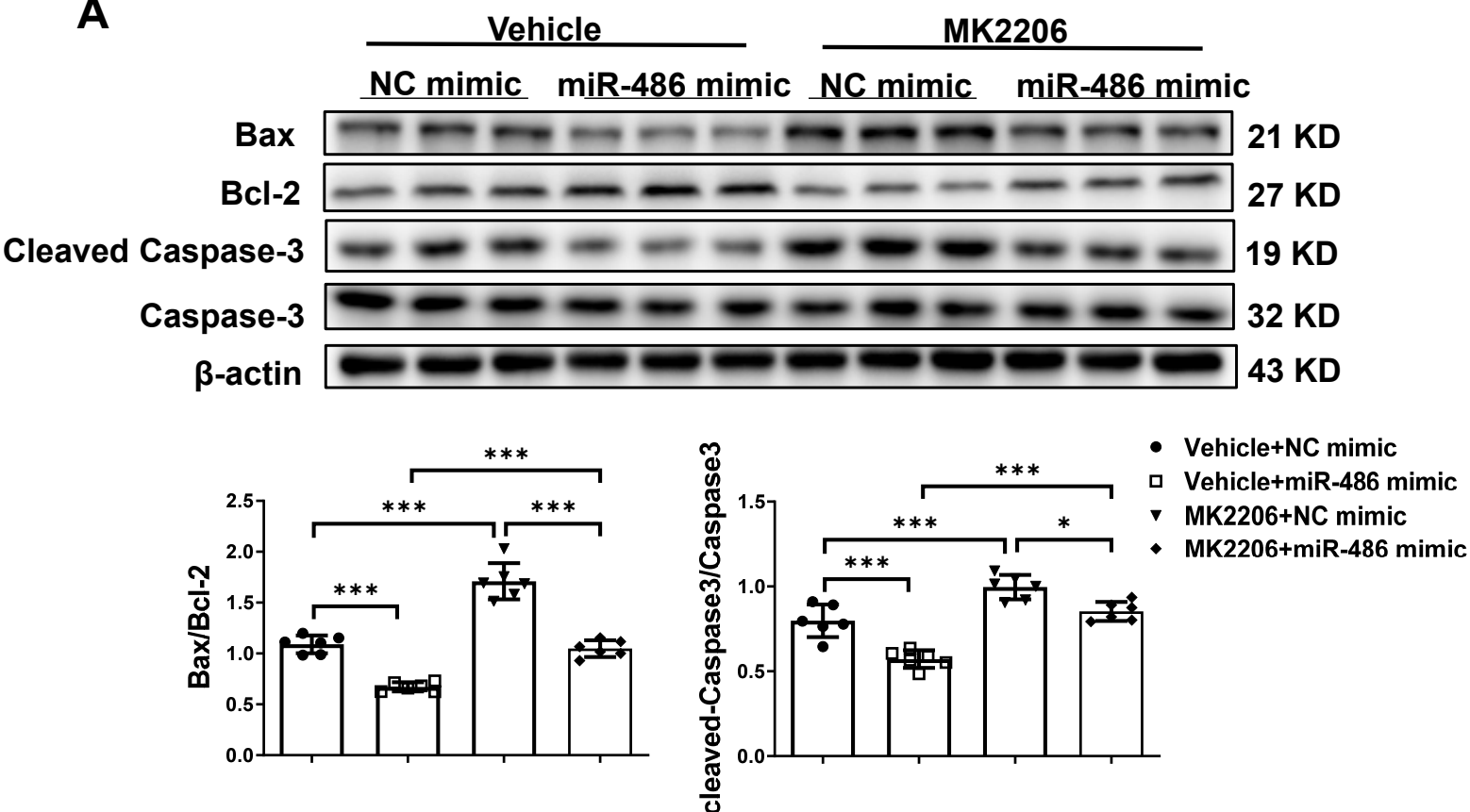


Figure S12

A



B

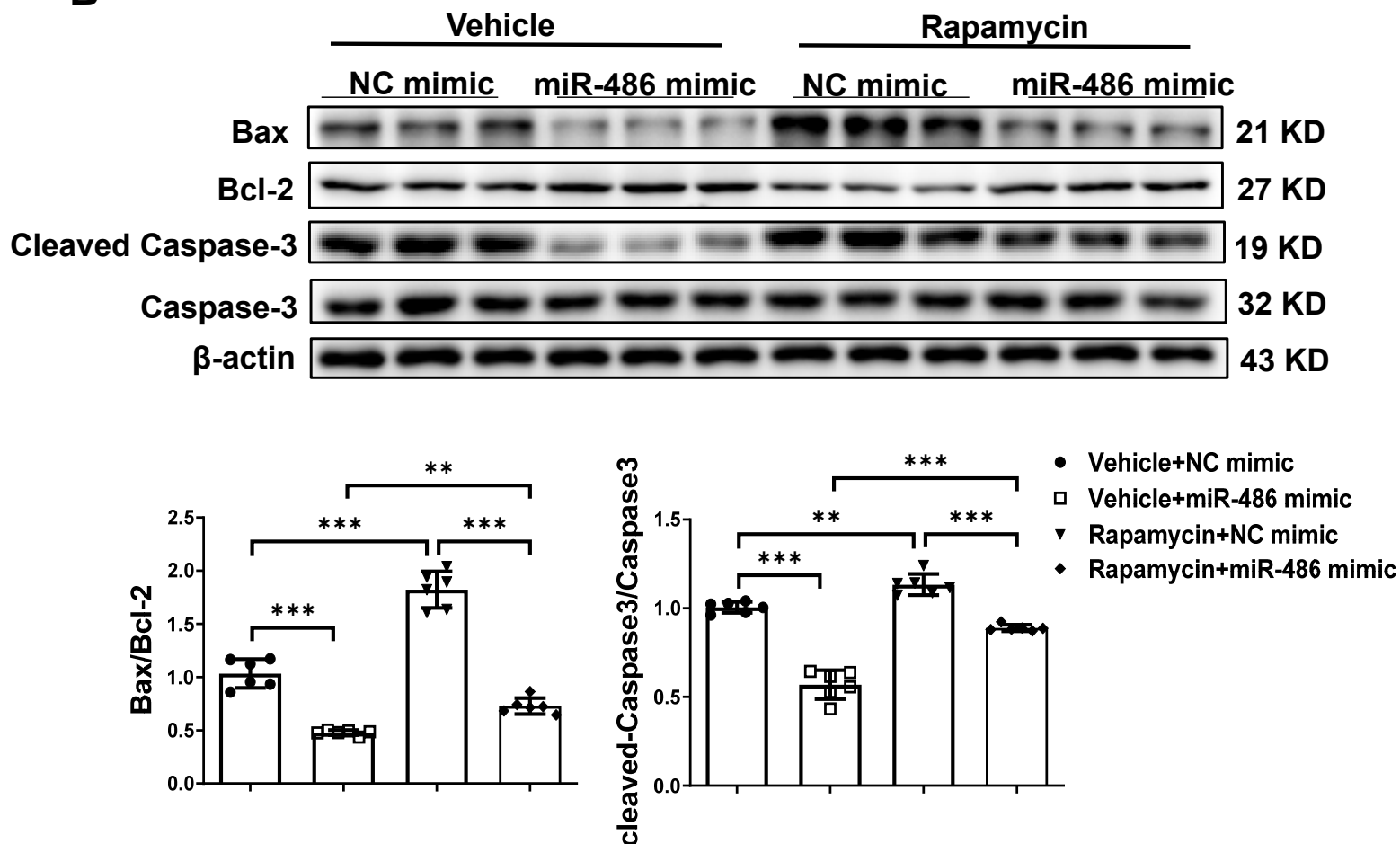
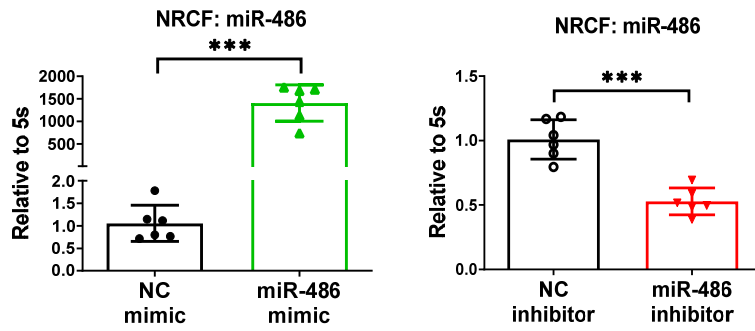
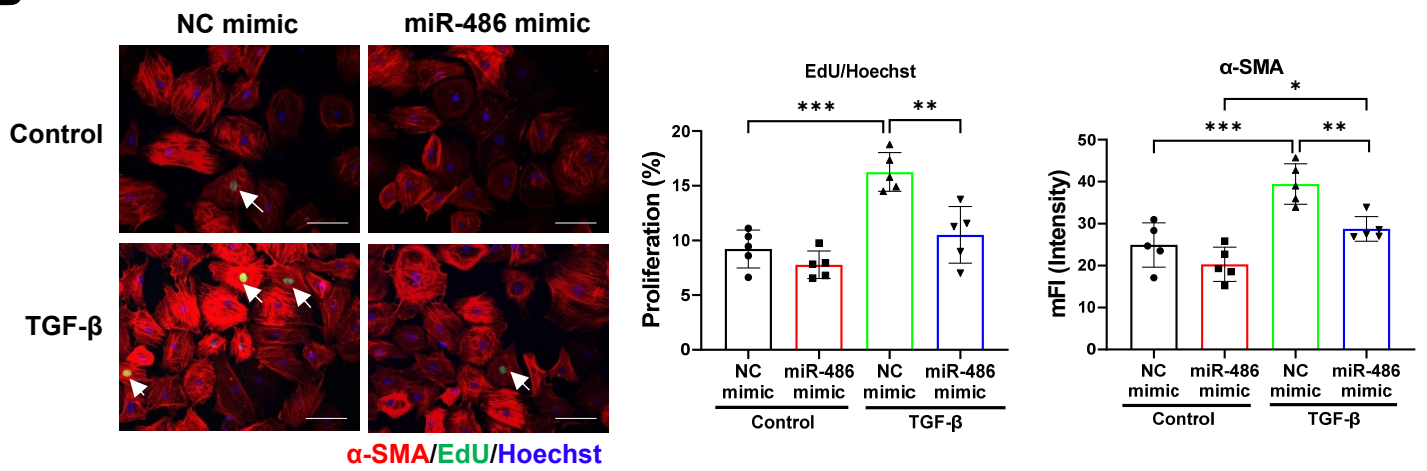


Figure S13

A



B



C

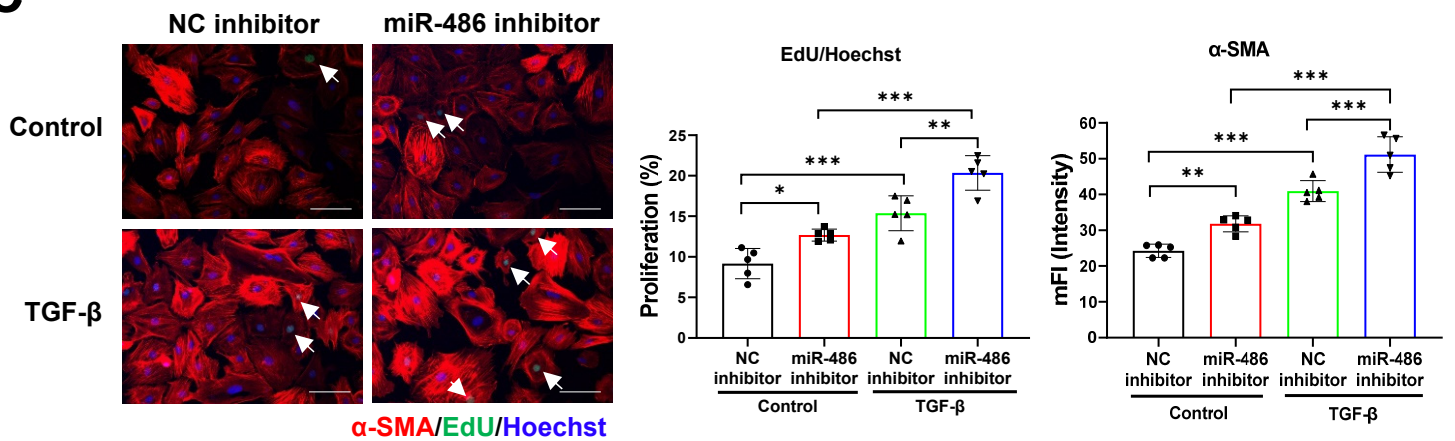
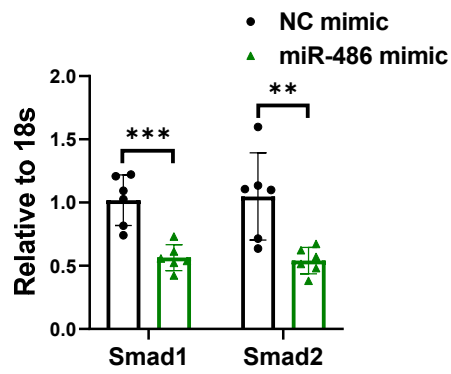
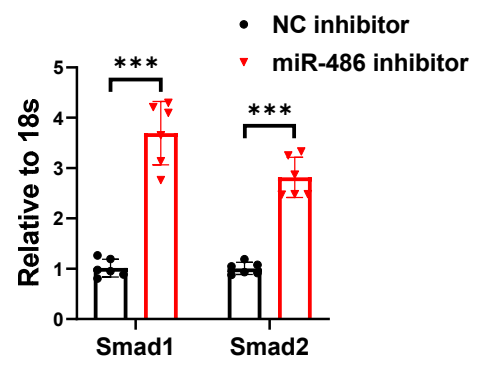


Figure S14

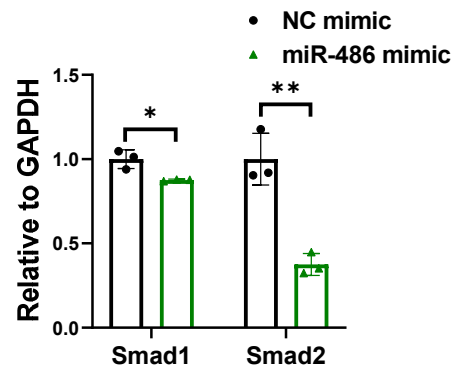
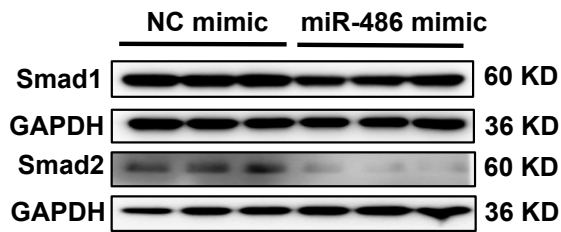
A



B



C



D

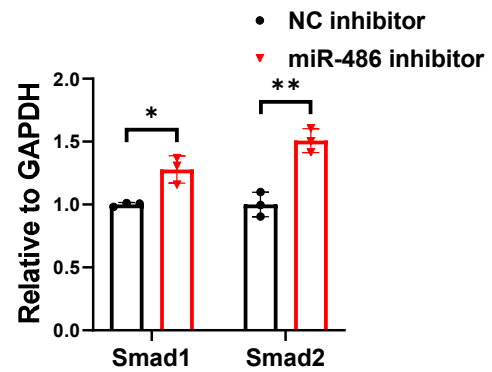
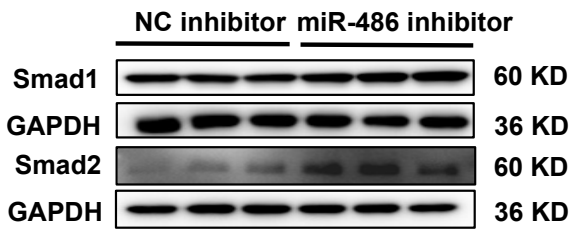


Figure S15

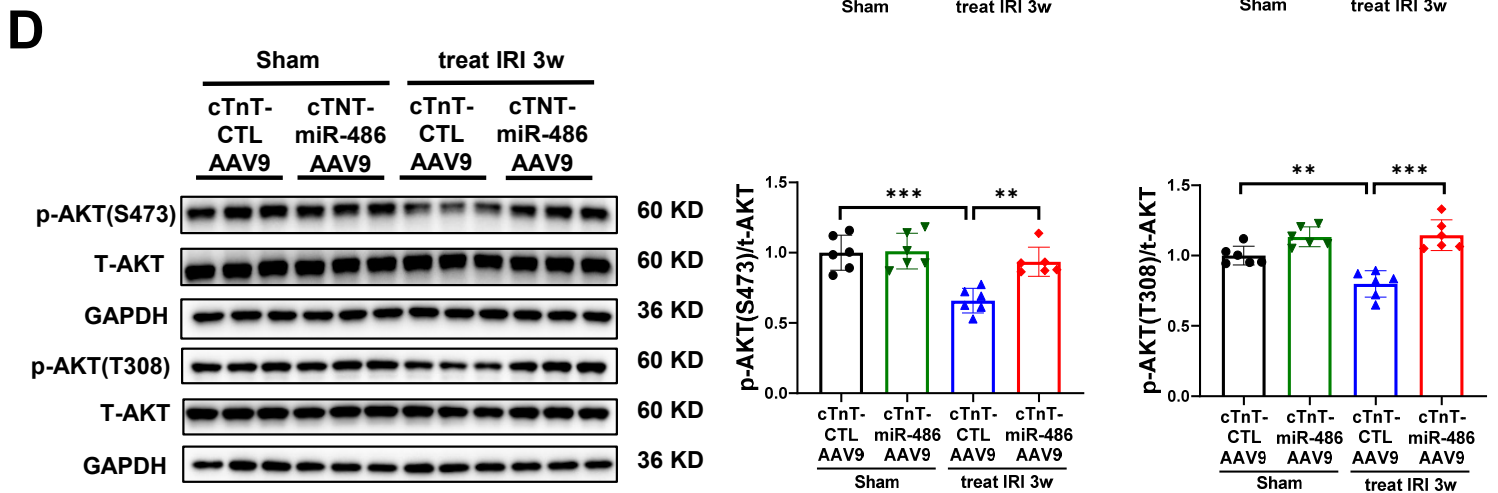
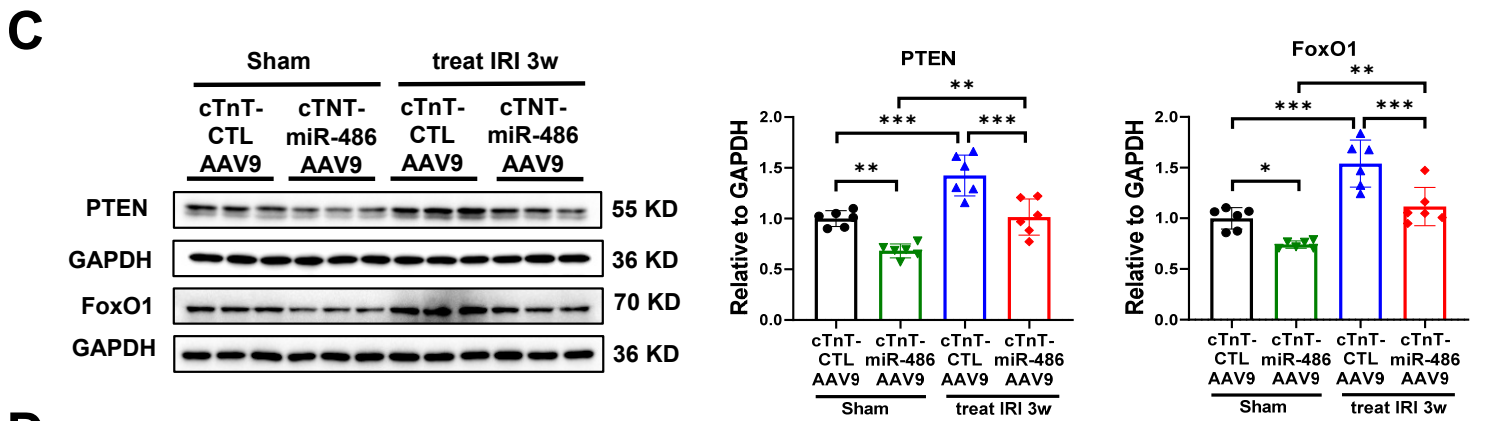
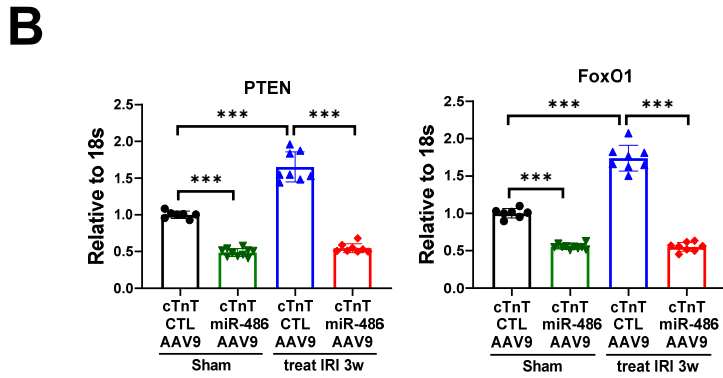
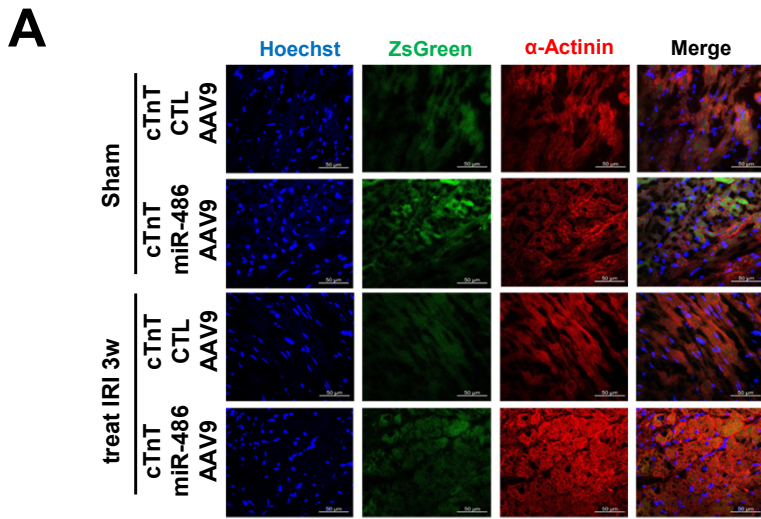


Figure S16

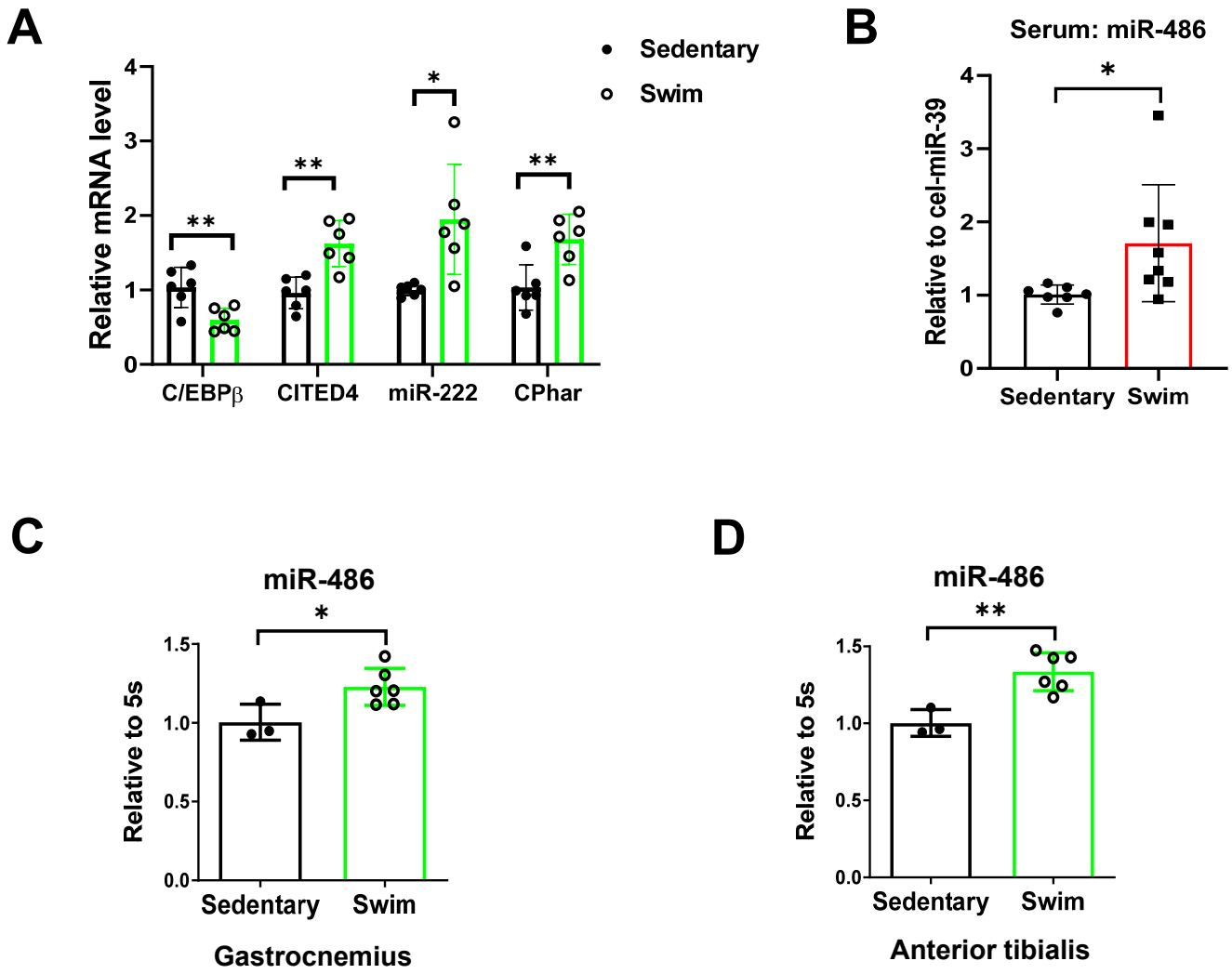
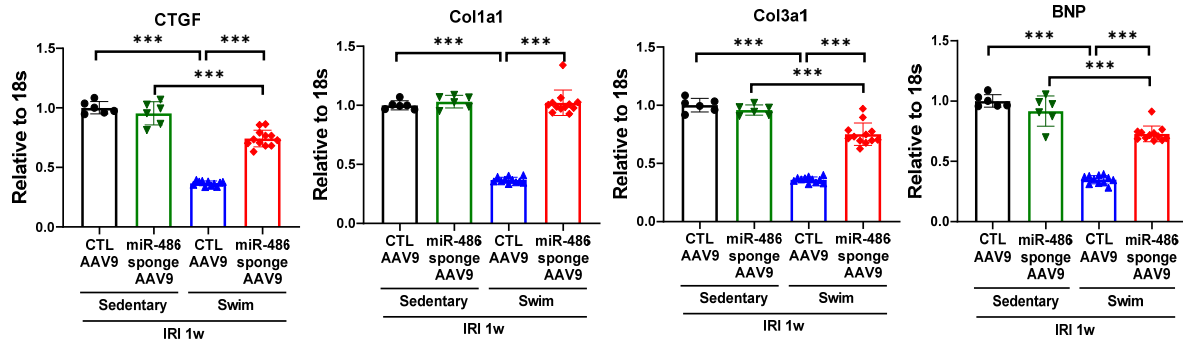


Figure S17

A



B

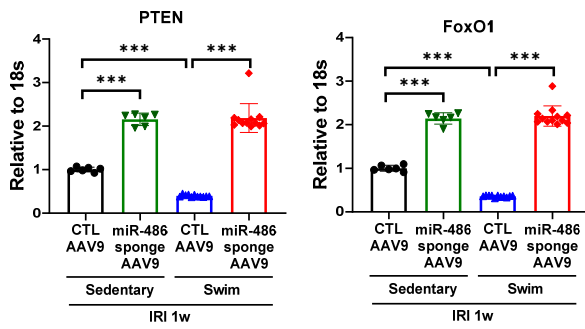
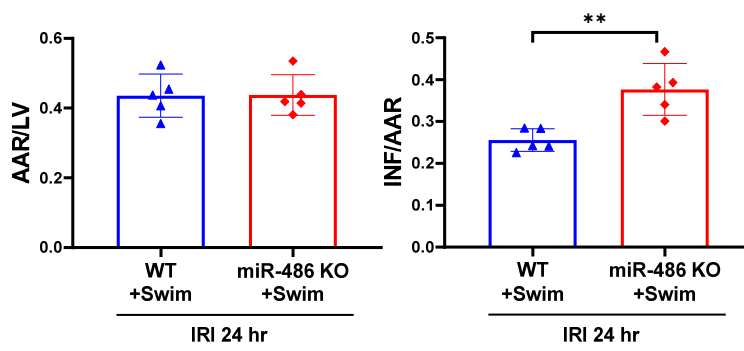
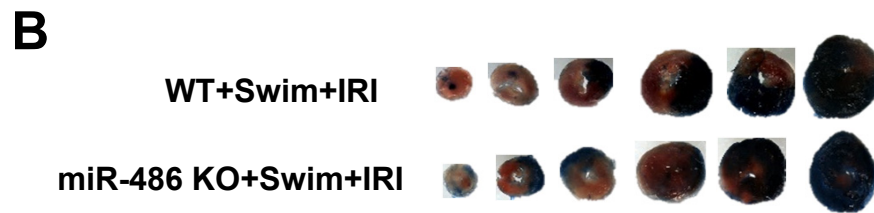
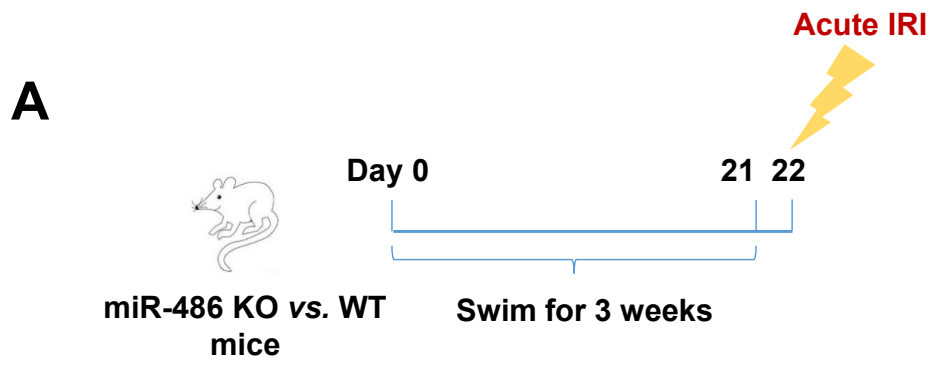


Figure S18



Supplemental Figure Legends

Figure S1. Preventive intervention by miR-486-AAV9 in acute cardiac ischemia/reperfusion injury. (A) Schematic diagram showing that AAV9 expressing miR-486 (miR-486-AAV9) or AAV9 controls (CTL-AAV9) were injected via tail vein, and 3 weeks later mice were subjected to cardiac ischemia/reperfusion (I/R) injury for 24 hrs. (B) RT-PCR for miR-486 expression in mice heart tissues at 24 hrs post cardiac I/R injury (n=6). (C) Western blot for Bax/Bcl-2 ratio and cleaved-Caspase3/Caspase3 ratio in mice heart tissues (n=6). (D) RT-PCR for CTGF, Col1a1, Col3a1, and BNP expressions in mice heart tissues (n=6). Data were compared by two-way ANOVA test followed by Tukey post hoc test. *, $P<0.05$; **, $P<0.01$; ***, $P<0.001$.

Figure S2. Preventive intervention by miR-486-AAV9 in chronic cardiac ischemia/reperfusion injury. (A) Schematic diagram showing that AAV9 expressing miR-486 (miR-486-AAV9) or AAV9 controls (CTL-AAV9) were injected via tail vein, and 1 week later mice were subjected to cardiac ischemia/reperfusion (I/R) injury for 3 weeks. (B) RT-PCR for miR-486 expression in mice heart tissues at 3 weeks post cardiac I/R injury (n=9-10). (C) Western blot for Bax/Bcl-2 ratio and cleaved-Caspase3/Caspase3 ratio in mice heart tissues (n=3). Data were compared by two-way ANOVA test followed by Tukey post hoc test. **, $P<0.01$; ***, $P<0.001$.

Figure S3. Long term protective effect of miR-486 overexpression against cardiac ischemia/reperfusion injury and cardiac dysfunction over 6 weeks. (A) Survival rate of mice injected with miR-486-AAV9 or CTL-AAV9 after 6 weeks of cardiac ischemia/reperfusion (I/R) injury (n=8,8,13,12 before I/R injury, n=8,8,10,12 at 6 weeks post I/R injury). (B) RT-PCR for miR-486 expression in mice heart tissues at 6 weeks post cardiac I/R injury (n=8-12). (C) Echocardiography for left ventricular

ejection fraction (EF, %) and fractional shortening (FS, %) in mice at 6 week after I/R injury (n=8-12). (D) Masson Trichrome staining for cardiac fibrosis in mice heart tissues (n=6-7). Scale bar=100 μ m. (E) RT-PCR for CTGF, Col1a1, Col3a1, and BNP expressions in mice heart tissues (n=8-12). Data were compared by two-way ANOVA test followed by Tukey post hoc test. **, $P<0.01$; ***, $P<0.001$.

Figure S4. Inhibition of miR-486 does not further aggravate cardiac ischemia/reperfusion injury. (A) The 2,3,5-triphenyltetrazolium chloride (TTC) staining for the infarct size at 24 hrs after cardiac ischemia/reperfusion (I/R) injury as determined by the infarct size/area at risk (INF/AAR) ratio. The area at risk/left ventricle weight (AAR/LV) ratio represents the homogeneity of surgery (n=6). (B) Schematic diagram showing that miR-486 sponge AAV9 or control AAV9 (CTL-AAV9) were injected via tail vein, and 1 week later mice were subjected to cardiac I/R injury for 3 weeks. (C) RT-PCR for miR-486 expression in mice heart tissues at 3 weeks post cardiac I/R injury (n=9-10). (D) Luciferase reporter assays performed in 293T cells co-transfected with negative control (NC mimic), miR-486 mimic or miR-210 mimic and the miR-486 binding site-carrying luciferase reporter plasmids (n=6). (E) Echocardiography for left ventricular ejection fraction (EF, %) and fractional shortening (FS, %) in mice at 3 week after I/R injury (n=9-10). (F) Masson Trichrome staining for cardiac fibrosis in mice heart tissues (n=6-7). Scale bar=100 μ m. (G) Western blot for Bax/Bcl-2 ratio and cleaved-Caspase3/Caspase3 ratio in mice heart tissues (n=6). (H) RT-PCR for CTGF, Col1a1, Col3a1, and BNP expressions in mice heart tissues (n=9-10). Data between 2 groups were compared by unpaired two-tailed Student's t-test. Data among 3 groups were compared by one-way ANOVA test. Data among 4 groups were compared by two-way ANOVA test followed by Tukey post hoc test. *, $P<0.05$; ***, $P<0.001$.

Figure S5. Transfection of miR-486 mimic or inhibitor in cardiomyocytes *in vitro*.

(A) RT-PCR for miR-486 expression in neonatal rat cardiomyocytes (NRCMs) transfected with miR-486 mimic, inhibitor, or negative controls (NC) (n=6). (B) Representative image of immunofluorescent staining for cardiac Troponin T (cTnT) which ensures the purification of human induced pluripotent stem cell-derived cardiomyocytes (hiPSC-CMs). Scale bar=100 μ m. (C) RT-PCR for miR-486 expression in hiPSC-CMs transfected with miR-486 mimic or negative control (n=4). (D) Relative hiPSC-CM numbers after oxygen glucose deprivation/reperfusion (OGDR) and transfection of miR-486 mimic (n=3). Data between 2 groups were compared by unpaired two-tailed Student's t-test. Data among 3 groups were compared by one-way ANOVA test. *, $P<0.05$; ***, $P<0.001$.

Figure S6. Regulation of PTEN and FoxO1 in human induced pluripotent stem cell-derived cardiomyocytes with miR-486 overexpression. RT-PCR for PTEN and FoxO1 in human induced pluripotent stem cell-derived cardiomyocytes (hiPSC-CMs) transfected with miR-486 mimic or negative control (NC mimic) (n=4). Data were compared by unpaired two-tailed Student's t-test.

Figure S7. Si-RNAs significantly downregulate PTEN or FoxO1 expression in neonatal rat cardiomyocytes. (A,B) RT-PCR for PTEN (A) or FoxO1 (B) expressions in neonatal rat cardiomyocytes (NRCMs) transfected with siRNAs targeting PTEN or FoxO1, respectively (n=4-6). Data were compared between PTEN or FoxO1 siRNA group and NC siRNA group using unpaired two-tailed Student's t-test. **, $P<0.01$; ***, $P<0.001$.

Figure S8. Western blot for Bax/Bcl-2 ratio and cleaved-Caspase3/Caspase3 ratio in oxygen glucose deprivation/reperfusion-treated neonatal rat cardiomyocytes transfected with miR-486 inhibitor and PTEN siRNA. (n=4). Data were compared

by two-way ANOVA test followed by Tukey post hoc test. **, $P < 0.01$; ***, $P < 0.001$.

Figure S9. Western blot for Bax/Bcl-2 ratio and cleaved-Caspase3/Caspase3 ratio in oxygen glucose deprivation/reperfusion-treated neonatal rat cardiomyocytes transfected with miR-486 inhibitor and FoxO1 siRNA. (n=6). Data were compared by two-way ANOVA test followed by Tukey post hoc test. *, $P < 0.05$; ***, $P < 0.001$.

Figure S10. Overexpression of PTEN or FoxO1 attenuates the protective effect of miR-486 mimic against cardiomyocytes apoptosis. (A,B) RT-PCR for PTEN and FoxO1 in neonatal rat cardiomyocytes (NRCMs) transfected with plasmids expressing PTEN (A) or FoxO1 (B) (n=6). (C,D) TUNEL staining for α -Actinin-labelled NRCMs transfected with miR-486 mimic and plasmids expressing PTEN (C) or FoxO1 (D) in the condition of oxygen glucose deprivation/reperfusion (OGDR) treatment (n=4). Scale bar=100 μ m. Data between 2 groups were compared by unpaired two-tailed Student's t-test. Data among 4 groups were compared by two-way ANOVA test followed by Tukey post hoc test. *, $P < 0.05$; **, $P < 0.01$; ***, $P < 0.001$.

Figure S11. Preventive delivery of miR-486-AAV9 regulates PTEN and FoxO1 in mice heart tissues. (A,B) RT-PCR (A) and Western blot (B) for PTEN and FoxO1 expressions in heart tissues from mice injected with miR-486-AAV9 before cardiac ischemia/reperfusion (I/R) injury. Heart tissues were harvested at 24 hrs post I/R injury (n=6). (C) Western blot for AKT phosphorylation levels in heart tissues from mice injected with miR-486-AAV9 before cardiac I/R injury. Heart tissues were harvested at 24 hrs post I/R injury (n=6). Data were compared by two-way ANOVA test followed by Tukey post hoc test. *, $P < 0.05$; **, $P < 0.01$; ***, $P < 0.001$.

Figure S12. MiR-486 inhibits cardiomyocyte apoptosis through activating AKT and mTOR. (A,B) Western blot for Bax/Bcl-2 ratio and cleaved-Caspase3/Caspase3 ratio in oxygen glucose deprivation/reperfusion (OGDR)-treated neonatal rat

cardiomyocytes transfected with miR-486 mimic in the presence or absence of AKT inhibitor MK2206 (A) or mTOR inhibitor Rapamycin (B) (n=6). Data were compared by two-way ANOVA test followed by Tukey post hoc test. *, $P<0.05$; **, $P<0.01$; ***, $P<0.001$.

Figure S13. MiR-486 inhibits cardiac fibroblast proliferation and activation. (A) RT-PCR for miR-486 in neonatal rat cardiac fibroblasts (NRCFs) transfected with miR-486 mimic, inhibitor, or negative controls (NC) (n=6). (B,C) Immunofluorescent staining for α -SMA/EdU in NRCFs transfected with miR-486 mimic (B), inhibitor (C), or NC (n=5). Scale bar=100 μ m. Data between 2 groups were compared by unpaired two-tailed Student's t-test. Data among 4 groups were compared by two-way ANOVA test followed by Tukey post hoc test. *, $P<0.05$; **, $P<0.01$; ***, $P<0.001$.

Figure S14. MiR-486 negatively regulates Smad1 and Smad2 in cardiac fibroblasts. (A,B) RT-PCR for Smad1 and Smad2 in neonatal rat cardiac fibroblasts (NRCFs) transfected with miR-486 mimic (A), inhibitor (B), or negative controls (NC) (n=6). (C,D) Western blot for Smad1 and Smad2 in NRCFs transfected with miR-486 mimic (C), inhibitor (D), or NC (n=3). Data were compared by unpaired two-tailed Student's t-test. *, $P<0.05$; **, $P<0.01$; ***, $P<0.001$.

Figure S15. Therapeutic delivery of cTnT-miR-486 AAV9 regulates PTEN and FoxO1 in mice heart tissues. (A) Immunofluorescent imaging for co-localization of ZsGreen (indicative of AAV9) and α -Actinin staining in heart tissues from mice injected with cTnT-miR-486 AAV9 or cTnT-control AAV9. Scale bar=50 μ m. (B,C) RT-PCR (B, n=7-10) and Western blot (C, n=6) for PTEN and FoxO1 expressions in heart tissues from mice treated with cTnT-miR-486 AAV9 within 30 min post myocardial reperfusion. Heart tissues were harvested at 3 weeks post cardiac ischemia/reperfusion (I/R) injury. (D) Western blot for AKT phosphorylation levels in

heart tissues from mice treated with cTnT-miR-486 AAV9 within 30 min post myocardial reperfusion. Heart tissues were harvested at 3 weeks post cardiac I/R injury (n=6). Data were compared by two-way ANOVA test followed by Tukey post hoc test. *, $P<0.05$; **, $P<0.01$; ***, $P<0.001$.

Figure S16. Expression of miR-486 in a mouse model of swimming exercise. (A) RT-PCR for the known factors in response to swimming exercise in heart tissues (n=6). (B) RT-PCR for circulating miR-486 levels in the serum from swimmable mice and sedentary mice (n=7-8). (C,D) RT-PCR for miR-486 expression in the gastrocnemius (C) and anterior tibialis (D) from swimmable mice and sedentary mice (n=3-6). Data were compared by unpaired two-tailed Student's t-test. *, $P<0.05$; **, $P<0.01$.

Figure S17. MiR-486 inhibition regulates fibrosis-associated gene markers and its downstream targets in swimmable mice upon cardiac ischemia/reperfusion injury. (A,B) RT-PCR for fibrosis-associated gene markers (A) and PTEN and FoxO1 (B) in mice heart tissues (n=6 for sedentary mice, n=11-12 for swimmable mice). Data were compared by two-way ANOVA test followed by Tukey post hoc test. ***, $P<0.001$.

Figure S18. The beneficial effect of swimming exercise against cardiac ischemia/reperfusion injury is attenuated in miR-486 knockout mice. (A) Schematic diagram showing that miR-486 knockout (KO) mice and wild type (WT) littermates were subjected to swimming exercise for 3 weeks before cardiac ischemia/reperfusion (I/R) injury for 24 hrs. (B) The 2,3,5-triphenyltetrazolium chloride (TTC) staining for the infarct size at 24 hrs after I/R injury as determined by the infarct size/area at risk (INF/AAR) ratio. The area at risk/left ventricle weight (AAR/LV) ratio represents the homogeneity of surgery (n=5). Data were compared by

unpaired two-tailed Student's t-test. **, $P < 0.01$.

Supplemental Table**Table S1. List of primers used for the PCR analysis.**

Gene	Primer sequence
rno_Pten forward	ATTGCCTGTGTGTGGTGA
rno_Pten reverse	TCCTCTGGTCCTGGTATGA
rno_FoxO1 forward	TGGGGCAACCTGTTCGTA
rno_FoxO1 reverse	GGGCACACTCTTCACCATC
mmu_Pten forward	AGCCCTAACCCCAAGAAC
mmu_Pten reverse	ACAAGTCCCGATGAAACCT
mmu_FoxO1 forward	GTACAGCGCATAGCACCA
mmu_FoxO1 reverse	GCGACAGACAGAGTTCCC
hsa_Pten forward	CAGTCAGAGGCGCTATGTGT
hsa_Pten reverse	CACCTTTAGCTGGCAGACCA
hsa_FoxO1 forward	GGATGTGCATTCTATGGTGTACC
hsa_FoxO1 reverse	TTTCGGGATTGCTTATCTCAGAC
mmu_C/EBP β forward	GGGGTTGTTGATGTTTTTGGT
mmu_C/EBP β reverse	TCGAAACGGAAAAGGTTCTCA
mmu_CITED4 forward	CCTGGCATAACGGCTCCTTC
mmu_CITED4 reverse	AGACTGCAGGTGCGTGCTAC
mmu_CPhar forward	CATGGATTTCTGGACCTCCTA
mmu_CPhar reverse	TTCATGGCTTTACAGCGT
rno_Smad1 forward	CGTGTTGGTGGATGGTTT
rno_Smad1 reverse	TGTGTCGCCTGGTATTTTC
rno_Smad2 forward	GTCAGTGCGATGCTCAAG
rno_Smad2 reverse	CTCAAGTGCTGTTTTTCGCT
mmu_CTGF forward	TAAGACCTGTGGGATGGG
mmu_CTGF reverse	GCAGCCAGAAAGCTCAA
mmu_Col1a1 forward	TAAGGGTCCCCAATGGTGAGA
mmu_Col1a1 reverse	GGGTCCCTCGACTCCTACAT
mmu_Col3a1 forward	CTGTAACATGGAAACTGGGGAAA
mmu_Col3a1 reverse	CCATAGCTGAACTGAAAACCACC
mmu_BNP forward	GAGTCCTTCGGTCTCAAGGC
mmu_BNP reverse	TACAGCCCAAACGACTGACG